

## Assessment of image quality and quantitative accuracy of point spread function (PSF)-based image reconstruction in Ingenuity Time of flight (TOF) PET/CT

<sup>1</sup>Sherif A. El Tamimy, MSc and <sup>2</sup>Magdy M. Khalil, PhD

<sup>1</sup>Sherif A. El Tamimy, MSc Nuclear Medicine and Radiation Oncology Center in Kasr Al-Ainy Hospital, Cairo University Hospitals, Cairo, Egypt.

<sup>2</sup>Magdy M. Khalil, PhD, Division of Medical Biophysics, Department of Physics, Faculty of Science, Helwan  
Corresponding Author: <sup>2</sup>Magdy M. Khalil, PhD,

### Abstract

**Aim.** Partial volume effect in positron emission tomography remains critical in image quality as well as quantitative accuracy especially in small oncologic lesions. Several attempts have been made to overcome this issue and improve the impact of partial volume on diagnostic accuracy of clinical PET imaging with no a universal consensus on a specific approach or method to follow. Introduction of point spread function in image reconstruction has proved useful in mitigating the impact of partial volume. The aim of this work was to investigate the role of point-spread-function (PSF) and regularization based reconstruction on image quality and quantitative accuracy using the commercially available Ingenuity time of flight PET/CT system.

**Methods.** Data were acquired using Jaszack phantom with fillable spheres of the diameters 9.89, 12.43, 15.43, 19.79, 24.82 and 31.27 mm. A number of clinically relevant image acquisitions was performed using different contrast ratio of 2:1, 5:1 and 10:1 as sphere to background ratio. Attenuation correction was carried out using the CT component of the scanner along with other necessary corrections of normalization, scatter, geometry, random events and dead time. Image reconstruction was performed using blob-based list-mode TOF reconstruction followed by PSF-based ML-EM deconvolution resolution recovery. The PSF-deconvolution was implemented at several combinations of PSF iterations (2,4,6,8,10,12) and regularization of 3,6, and 9 mm.

**Results.** The average error of SUVmax in all spheres was less than 10% has been achieved when using (PSF-regularization) of (2,3), (2,6), (2,9) (4,3), (4,9), (6,3), (6,6) and (6,9) at contrast ratio of 2:1 whereas the same level of error was achieved with only (2,3) at contrast ratio of 10:1. On the other hand, the average error of SUVmean was less than 10% in all spheres when using (PSF-regularization) of (6,9), (8,6), (8,9), (10,6), (10,9), (12,6), (12,9) at contrast ratio of 2:1 whereas (PSF-regularization) of (6,9), (8,6), (8,9), (10,6), (10,9), (12,6), (12,9) at contrast ratio of 5:1. At contrast ratio of 10:1, the (PSF-regularization) was (2,6), (2,9), (4,6), (6,6).

**Conclusion.** The number of PSF iterations combined with the regularization (smoothing) level of the reconstructed PET image play a significant role in the accuracy of the SUVmax as well as SUVmean determination. SUVmax tends to be more accurate at different number of iterations as well as regularization levels while the SUVmean tends to be more accurate at higher number of iterations with slightly higher smoothing levels. These findings would impact significantly on selection of reconstruction parameters in terms of which SUV metric to use and the level of resolution and smoothing kernels employed.

Date of Submission: 09-11-2017

Date of acceptance: 25-11-2017

### I. Introduction

Image quality improvement in PET images is under continued progress and development of PET system manufacturers. Reconstruction algorithm is a very important component to improve image quality hence the detectability of PET/CT is function of image formation.

A Number of several manufacturers have introduced time-of-flight (TOF) and point-spread function (PSF) algorithms that improve signal-to-noise ratios (SNRs) in conjunction with iterative reconstruction including the mostly commonly used ordered subsets expectation maximum (OSEM) algorithms [1,2].

In conventional PET, counts are evenly spread in pixels along the LOR, whereas in TOF PET, each pixel along the LOR is incremented by a probability on the basis of the arrival time of the annihilation photons [17]. TOF PET is facilitated by using cerium-doped lutetium orthosilicate or lutetium–yttrium orthosilicate scintillation crystals (LYSO), which improves timing resolutions. TOF reconstruction has been proven in several studies to improve signal to noise ratio as well other image quality metrics [ ]. Conclusion PSF reconstruction significantly improved image quality for both clinical and phantom studies. It also served to improve image quality, lesion detection , CNR, SNR, FWHM particularly in larger tumors or area [2].

In PET, the spatial resolution is limited by the size of the crystal element [18,26]. Photons produced in the center of the scanner are detected and localized correctly; however, photons produced towards the edge of the field of view (FOV) are more likely to be localized incorrectly; the photon strikes the crystals at an angle and is therefore likely to travel to a neighboring crystal, contributing towards a spatial distortion [3].

**The point spread function (PSF)** describes the response of an imaging machine to a point source or point object. A more general term for the PSF is a system's impulse response, the PSF being the impulse response of a very small (spatial) input function. The PSF in many contexts can be thought of as the extended blob in an image that represents an unresolved object. PSF reconstruction produces images with improved isotropic spatial resolution, reduced spill-in/spill-out, and ultimately increased activity concentration (Bq/mL) or standardized uptake value (SUV) in small lesions. These benefits have been demonstrated as higher recovery coefficients (RCs) in NEMA phantom studies [3] and improved lesion detectability in patient studies [4].

The aim of the study was to find out the best combination of the PSF number of iterations and the regularization level of the final reconstructed PET images. This has been evaluated in terms of the most commonly used SUV metrics including SUV<sub>max</sub> and SUV<sub>mean</sub> at significantly wide dynamic range of target to non-target ratio of 2:1, 5:1, and 10:1.

## **II. Materials and Methods**

### **A. Phantom Acquisition**

A Jaczack phantom with 6 fillable sphere was used in the study. The Jaczack cylindrical phantom weighed 8.3 kg and manufactured from polymethylmethacrylate material with the hot spheres having inner diameter of 9.89, 12.43, 15.43, 19.79, 24.82 and 31.27 mm. It has a cylinder inside diameter of 216 mm, inside height of 186 mm as well as wall thickness of 3.2 mm.[8,9]

During the filling phantom process, different lesion to background ratio of 2:1, 5:1, 10:1 was considered as it could represent real life scenario of adequate wide dynamic range of various malignancies. The time per bed position was 3 min/bed in list mode identical to the time that is used routinely in our clinic. The total activity measured in all spheres was 31.5 ml accounting for 600 nCi/ml total activity. The activity in the background was almost 300 nCi/ml, 120 nCi/ml and 60 nCi/ml for the above mentioned three contrast ratio.

After careful filling of the phantom as well as the background, a clinically relevant data acquisition was performed using the whole body acquisition protocol used in our patient's workflow. Acquisition commenced immediately post phantom preparation with proper laser alignment of the sphere being centered in the axial and trans-axial field of view. Image reconstruction was performed using the Philips Ingenuity 64 PET/CT system with TOF enabled using several combinations of point spread function iterations and regularization levels. The imaging system is summarized in table 1 while table 2 summarizes the PSF-regularizations used in the study.

The Attenuation correction was carried out using the CT component of the scanner along with other necessary corrections of normalization, scatter, geometry, random events and dead time. Image reconstruction was performed using blob-based list-mode TOF reconstruction followed by PSF-based ML-EM deconvolution resolution recovery. The PSF-deconvolution was implemented at several combinations of PSF iterations (2,4,6,8,10,12) and regularization of (3,6, and 9) mm producing a total number of 18 reconstructed image per each contrast ratio in addition to the disabled PSF reconstruction. The PET imaging field of view was 576 and reconstruction matrix of 288\*288.

Data were then transferred to the processing workstation for reconstruction and data visualization. The scatter correction was the single simulation approach and the attenuation correction utilized the information obtained from the CT data set. The CT component of every acquisition was identical to real patient data where the tube current was 118 mA and tube voltage of 120 kVp, slice thickness of 1.5 mm producing image dimensions (X, Y, Z): 512 x 512 x 149. The axial extension was 18 cm.

### **B. Image analysis and processing.**

After image reconstruction using the above mentioned reconstruction parameters, quantitative measurements were performed using region of interest analysis by placing a well-defined ROI placed over every sphere such that 70% of the sphere is occupied by the ROI size, as illustrated in figure (3-1). The mean SUV (SUV<sub>mean</sub>), maximum SUV (SUV<sub>max</sub>), standard deviation were recorded for every measurement taken on the radioactive spheres. The % error was measured for SUV<sub>max</sub> as well as SUV<sub>mean</sub> provided the fact that the true value is known beforehand. The formula  $(\text{True}-\text{Measured})/\text{True} \times 100$  was used as measure of the % error in measurements. We also calculated the average percentage error for the smallest 3 hot spheres for SUV<sub>mean</sub> and SUV<sub>max</sub> as well as percentage error for the smallest hot sphere again for both SUV variants.

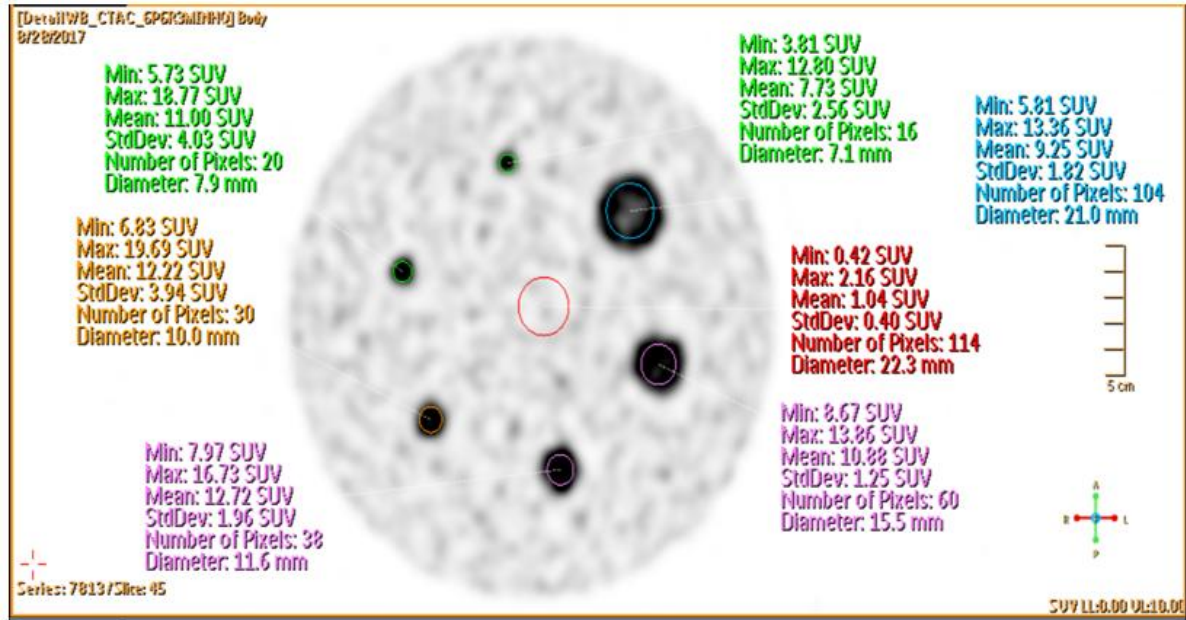


Figure 1. illustrate the ROI analysis method used in data quantitation and determination of SUVmax, SUVmean, SUVsd, and SUVmin.

### III. Results

The average error of SUVmax in all spheres was less than 10% has been achieved when using (PSF-regularization) of (2,3), (2,6), (2,9), (4,3), (4,9), (6,3), (6,6) and (6,9) at contrast ratio of 2:1 whereas the same level of error was achieved with only (2,3) at contrast ratio of 10:1, as shown in table 1. On the other hand, the average error of SUVmean was less than 10% when using (PSF-regularization) of (6,9), (8,6), (8,9), (10,6), (10,9), (12,6), (12,9) at contrast ratio of 2:1 whereas (PSF-regularization) of (6,9), (8,6), (8,9), (10,6), (10,9), (12,6), (12,9) at contrast ratio of 5:1. At contrast ratio of 10:1, the (PSF-regularization) was (2,6), (2,9), (4,6), (6,6), as demonstrated in table 2.

Table (1): The psf-reg combination that revealed an error of less than 10% in SUVmax

		All spheres	3 Smallest Spheres	Last sphere
1	2 : 1	(2,3) , (2,6) ,(2,9) ,(4,3) ,(4,6) ,(4,9) ,(6,3),(6,6) ,(6,9)	(4,3) , (6,3) ,(6,6) ,(8,3) (8,6) ,(10,3) ,(10,6),(12,3),(12,6) ,(12,9)	No
2	5 : 1	No	No	No
3	10 : 1	(2,3)	(2,3)	No

Table 2. The psf-reg combination that revealed an error of less than 10% in SUVmax

		All spheres	3 Smallest Spheres	Last sphere
1	2 : 1	(6,9) , (8,6) ,(8,9) ,(10,6) , (10,9) , (12,6) , (12,9)	NO	NO
2	5 : 1	(6,9) , (8,6) , (8,9) , (10,6) , (10,9) ,(12,6),(12,9)	(10,9) , (12,6) , (12,9)	No
3	10 : 1	(2,6) , (2,9) ,(4,6) , (6,6) ,	(4,6) , (4,9) , (6,6) , (6,9) ,	(12,9) ,

#### IV. Discussion

Partial volume correction is one of the most important elements in quantitative PET imaging. Several attempts have been made to resolve this issue with particular emphasis placed on quantitative accuracy and its implication in diagnostic and therapeutic regimens. Several factors contribute to the resolution limits of the reconstructed PET data including positron range, non-collinearity, crystal dimension as well other reconstruction parameters such as type of reconstruction algorithms, number of iterations, number of subsets (in case of MLEM and OSEM type reconstruction) or penalty prior;  $\beta$ , as in maximum a posteriori type reconstruction (Bayesian based approach). Partial volume can be quantitatively corrected using simple measurements of objects at different physical sizes that extends from few millimeters up to two or three times the spatial resolution of the system (2-3 FWHM).

The Ingenuity PET/CT employs blob-based list-mode TOF reconstruction followed by PSF-based MLEM de-convolution resolution recovery. The deconvolution approach makes use of the point spread function which can be estimated from data measurements taken for the system at large number of spatial points within the scanner field of view. It could potentially improve the quantitative measurements of the acquired PET data but at increased noise levels. Contrast-noise ratio is an image quality index that must be controlled so that a good balance between the two measures is maintained. In this study, the attempt was to look for the best combination of the contrast noise balancing ratio that is determined by the increased number of iterations (improve spatial resolution) and the filtration step that serve to reduce the sharpness of the resulting images.

At low contrast ratio (i.e. 2:1), there were several combinations between the PSF iterations and the regularization level such that the average error in SUVmax measurements was less than 10%. However, at higher contrast ratio there were minimal success to get the same level of error except with 2 iterations and regularization of 3 mm at contrast ratio of 10:1. Taking the error of the three smallest spheres for the SUVmax didn't show a better error level in comparison to whole spheres evaluation. Furthermore, the error level was even more than 10% in the smallest sphere size. The later finding was the same in all contrast ratios and in all combinations of the PSF and regularization levels.

For SUVmean measurements, again there were several combinations of the PSF iterations and regularization that achieved similar error levels to SUVmax especially at lower contrast ratio but with better performance in medium and high contrast ratios. There was an adequate number of combined (PSF-regularization) that could achieve an acceptable error levels (i.e <10%) but with remarkable increase in the smoothing kernel of the resolution recovery algorithm. This was also so evident in the smallest sphere of the phantom provided that the PSF iteration number was 12 and the smoothing level was at 9 mm compromising the quality of the reconstructed data.

At the smallest three spheres, the SUVmean was maintained stable through few combinations of the (PSF-regularization) such that the average error was less than 10% in medium and high contrast ratio but not in 2:1 activity concentration. This came at the expense of increasing the value of (PSF-regularization) combinations improving the SUVmean in the higher contrast ratio 10:1 rather than the moderate one 5:1. For the smallest sphere, there was a noticeable improvement in the SUVmean with error less than 10% but this was traded-off with increased image smoothing. It was also noticed that higher contrast ratio require less number of PSF iterations in comparison to low and medium activity concentrations. This was obtained to the extent that the combinations (12,9) was able to provide the same level of error in the smallest sphere at the highest contrast ratio considered. Again, this came at the extent of increasing image smoothness and reduced image quality.

#### V. Conclusions

The number of PSF iterations combined with the regularization (smoothing) level of the reconstructed PET image play a significant role in the accuracy of the SUVmax as well as SUVmean determination. SUVmax tends to be more accurate at relatively low number of iterations as well as regularization smoothing levels while the SUVmean tends to be more accurate at higher number of iterations with slightly higher smoothing levels. These findings would impact significantly on selection of reconstruction parameters in terms of which SUV metric to use and the level of resolution and smoothing kernels employed.

#### Reference

- [1]. Gopal B. Saha, PhD Basics of PET Imaging Physics, Chemistry, and Regulations ,2004.
- [2]. Lynch T.B: PET/CT in Clinical Practice.,1<sup>st</sup> edition (10-29,204-206),2007.
- [3]. O. L. Munk1\*, L. P. Tolbod1, S. B. Hansen1 and T. V. Bogsrud1,2 Point-spread function reconstructed PET images of sub-centimeter lesions are not quantitative, 2017.
- [4]. Jianhua Yan, Josh Schaefferkoetter, Maurizio Conti and David Townsend A method to assess image quality for Low- dose PET: analysis of SNR, CNR, bias and image noise 3,4 , 2016.
- [5]. Taisuke Murata, Kenta Miwa, et al: .Evaluation of spatial dependence of point spread function-based PET reconstruction using a traceable point-like 22Na source , 2016.
- [6]. H Zaidi1, N Ojha, M Morich, et al.; Design and performance evaluation of a whole-body Ingenuity TF PET-MRI system , 2016.

- [7]. Nicholas J. Vennarta,b, Nicholas Birda, et al: Optimization of PET/CT image quality using the GE ‘Sharp IR’ point-spread function reconstruction algorithm. 2017.
- [8]. Philips Ingenuity PET/CT 64 TF user manual, 2011.
- [9]. Ingenuity Data Acquisition and Sampling , Philips healthcare Company , 2014.
- [10]. Perkins A, Stearns C, Chapman J, et al : NEMA (National Electrical Manufacturers Association) Standards Publication Performance Measurements of Positron Emission Tomographs, 2007.

Sherif A. E Assessment of image quality and quantitative accuracy of point spread function (PSF)-based image reconstruction in Ingenuity Time of flight (TOF) PET/CT.” IOSR Journal of Applied Physics (IOSR-JAP) , vol. 9, no. 6, 2017, pp. 43-47.